2006 Symposium on Haptic Interfaces For Virtual Environment And Teleoperator Systems
IEEE VR, Arlington, VA, 25-26 March 2006. pp. 67-72.

Compact, Portable, Modular, High-performance, Distributed Tactile Transducer Device Based on Lateral Skin Deformation

Qi Wang* and Vincent Hayward†
Haptics Laboratory, Center for Intelligent Machines
McGill University, Montréal, Québec, Canada

ABSTRACT

We describe a tactile transducer system that has a compact, yet modular design. The tactile transducer comprises a 6×10 piezo bimorph actuator array with a spatial resolution of 1.8×1.2 millimeter and a wide temporal bandwidth. The blocked force of individual actuators can be changed (0.15 N, 0.22 N) by adjusting the cantilever mechanics to optimally match skins and/or applications. This tactile transducer is modular, appeals to ordinary fabrication methods, and can be assembled and dismantled in a short time for debugging and maintenance. It weighs 60 g, it is self-contained in a 150 cm^3 volume and may be interfaced to most computers, provided that two analog outputs and six digital IO lines are available. A pilot test was carried out where subjects were asked to detect a virtual line randomly located on an otherwise smooth virtual surface.

CR Categories: H.5.2 [Information Interfaces and Presentation]: User Interfaces—Haptic I/O; H.5.1 [Information Interfaces and Presentation]: Multimedia Information Systems—Artificial, augmented, and virtual realities

Keywords: tactile displays, haptic devices, virtual reality

1 INTRODUCTION

Tactile displays are meant to create computer-generated tactile sensations similar to those arising when holding objects, palpating them, or sliding fingers on their surfaces. The design and the fabrication of transducers for these displays have received quite a bit of attention from researchers, despite the difficulties encountered in achieving systems which are robust, effective, manufacturable, and of reasonable complexity.

This problem has been approached in various ways. Attempts have been made to leverage the benefits of smart actuators (shape memory alloy wires or springs [24, 20], miniature electrostatic actuators [8], electroactive gels [11]), specifically developed technologies (pneumatic bladders [14], miniature electromagnetic solenoids [9]), consumer-oriented modules for the toy industry [21], or "remotized" miniature DC motors [16].

Another direction of investigation is characterized by experimention with techniques for interaction with the skin that include tapping on it [2], vibrating it [17], brushing against it [5], electrostatic adhesion [18], slip [23], or ultra-sonic pressure [7].

In the past few years, our group has been developing several tactile transducers which use the principle of deforming the skin by tangential traction [6]. The idea is to design a display system that *produces skin deformations* which resemble those experienced by the fingerpad skin during contact with objects *rather than attempting to re-create the cause* of these deformations. Recently, there has been increasing evidence of the effectiveness of this approach to create the experience of small shapes [13], or surface undulation [10]. At the same time skin lateral deformation is being studied for its perceptual contributions to the design of transducers [1, 4, 19].

This paper describes a high performance tactile transducer device which improves on the STReSS device described in [15], which, in turn, was a significant improvement over that described in [6]. These developments are motivated by the assiduous pursuit of complexity reduction, both in the fabrication and the assembly methods, while boosting performance.

The specific aim of this project was to design and build a compact, high performance, low-power, modularized tactile transducer. We adopted a practical approach in this process: we did not seek to develop new actuator technology, nor any new fabrication method. Yet, we strived not to to compromise performance and sought to minimize complexity to the greatest extent possible (in number of parts, fabrication of parts, and assembly time).

2 DESIGN EVOLUTION

Figure 1 summarizes the main characteristics of the three successive designs which are characterized by increasing performance and diminishing complexity.

2.1 Electromechanical Architecture

In the initial design represented in the top row of the figure, a dense array of piezoelectric actuators arranged vertically operated in d_{31} mode (electric field applied laterally, mechanical deformation along the vertical direction). The actuators were bonded to a deformable membrane with specific elastic characteristics to allow for its local deformation. This allowed the vertical tubes bonded to the upper surface of the membrane to swing laterally in two directions. The main difficulties encountered with this device were the fabrication of the membrane and the assembly of all the parts. While these were overcome, the intensity of the tactile images were too low to be generally useful. This was due to the compliance of the structure and the limited free deflection of the contactors.

This led us to consider the "stacked comb" design of the STReSS device illustrated in the second row of Figure 1. Actuators were now fabricated by sets of ten out of solid bimorph piezoelectric plates (Y poled), which greatly simplified assembly. While this design allowed us to verify that, indeed, when deformation patterns are created on the skin with millimetric scale resolution, the exact characteristics of the local strain did not seem to make a difference on the resulting conscious experience, only large scale patterns mattered. Despite significant improvement in the intensity of the stimuli, these were still found too weak for the average user. Also the device assembly was hard due to the numerous electrical connections that had to be made in small space.

But perhaps the greatest problem was robustness. Should one or several actuators be damaged or fail, the entire device had to be reconstructed from scratch.

*email: qiwang@cim.mcgill.ca
†email: hayward@cim.mcgill.ca

In this paper, we introduce a new architecture shown in "exploded view" in the bottom row of Figure 1. Now each actuator module can be manufactured separately and plugged onto two lateral printed circuit boards which provide both electrical connections and structural strength. In effect, we found that the cantilever mechanics of commercially available piezoelectrical bimorphs were not sufficient to create the desired skin deformation [22]. Later in this paper we will describe a new technique that modifies the basic compliance-deflection tradeoff of piezoelectric benders and which allows for reasonable activation voltages.

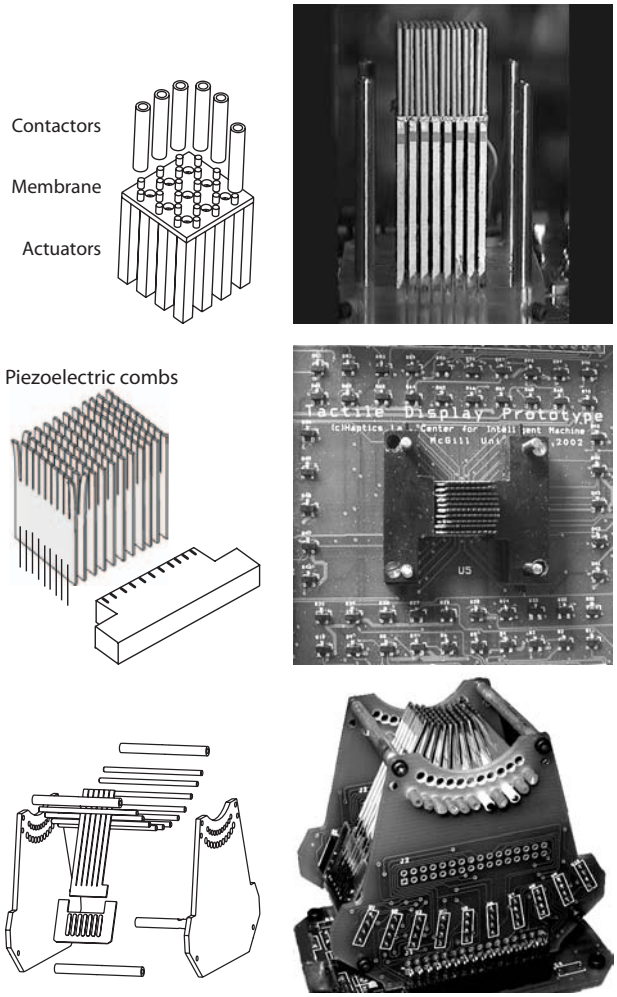

Figure 1: Top row: Membrane architecture described in [6]. Middle row: STRESS architecture as in [15]. Bottom row: Modular design as in this paper. To give scale, in all cases the active surface is about 1 cm^2.

2.2 Driving Electronics

Supplying control signals to a large number of high-voltage channels is a problem that has many tradeoffs. These tradeoffs are driven by the necessity to route many wires at various stages the chain from the digital representation of signals to the final delivery of power to each actuator. In Figure 2, the three successive designs that we have explored are schematically represented. Each has a particular set of advantages and drawbacks which are briefly discussed now.

In the top panel of the figure, multiplexing was achieved thanks to fast, high-voltage opto-electronic switches. Actuators were organized in rows and columns. Each column of actuators was written in parallel with $N = 8$ analog amplifiers and $M = 8$ columns were multiplexed using one opto-electronic switch for each actuator. In essence, it was a cross-bar design with the sample-and-hold function accomplished by the switches and the actuators themselves (essentially capacitors). This architecture offers what essentially amounts to an overall compromise in components count and width of analog and digital buses. The cost of the opto-electronics was the main drawback.

A second design explored with the STRESS device took advantage of the PWM signal representation to essentially eliminate analog signals until the very end of the chain. Since the logic was much more complex, it was implemented in an FPGA chip. This offered much flexibility in that it was possible to off-load some low-level functions from the host computer. This also allowed for readily available USB connectivity. One significant drawback is the delay incurred in transmitting tactile frames. Also, the design of the power stage was difficult, especially when implemented with a single active component switch, as was done for the STRESS device.

In the present design (bottom panel of Figure 2), we took advantage of the recent availability of a multiple channel chip designed primarily for driving highly parallel MEMS devices, which, clearly, is a problem similar to ours. In this device, the sample-and-hold function for multiplexing the analog signal is integrated in the chip itself. One disadvantage of this design is the difficulty in commissioning the chip which requires careful sequencing of supply voltages during power cycling. Also, in case of accidental destruction of one channel, an entire chip has to be replaced.

We have experimented with several other circuit architectures, each with its own set of advantages and drawbacks which would be meaningful to discuss only in the context of specific applications.

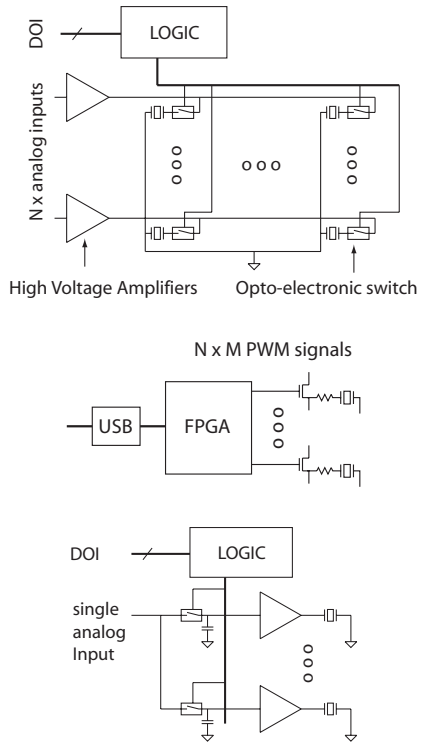

Figure 2: Top panel: Electronic design of the device described in [6]. Middle panel: Electronic design of the device described in [15]. Bottom panel: Design as in this paper.

3 DESIGN GOALS

The general design goals did not depart from what is often desired for such transducers, save for fact that the principle of operation is to apply tangential traction to the skin, rather than normal indentation. Specifically these goals were:

- **Modular design**. Researchers who have attempted the design and construction of high density transducers have often commented on the necessity to leave room for experimentation and debugging. Therefore a key requirement for an experimental design is modularity as well as assembly/disassembly convenience.

- **Compact and light-weight**. It is also often commented that good prospects for applications of tactile displays come from their ability to be integrated with force-feedback haptic devices, or by association with conventional data input devices, or yet by being directly worn with, for example, a data glove. As such, bulk and weight are key factors. This also holds true for the driving electronics, lest the user be forced to cope with cumbersome cable bundles.

- **Large skin deformation**. Specifications for pin-type transducers are often described in terms of pin displacement and exerted force. The intricate details of contact mechanics created by millimetric-scale skin contactors preclude simple descriptions in terms of their intrinsic effects on the skin. In contrast, for tangential traction transducers, these specifications are more straightforward since the objective is create deformation in small patches defined by the geometry of the contactors. Direct in vivo measurements [12], informal observations [13], as well as recent biomechanical data [22] lead us to believe that the target tangential skin deformation could be in the range of 30%.

- **Wide bandwidth**. It is generally accepted that a general purpose tactile transducer system requires wide bandwidth since the skin is known to repond to high-frequency signals (a few hundred Hz according to the stimulation conditions).

- **High spatial resolution**. It is also well accepted that the target spatial period of the transducer should be lower than 2 mm.

4 SYSTEM FABRICATION

4.1 Tactile transducer

The present configuration of the tactile transducer comprises 60 miniature piezo bimorph blades forming a 6×10 array. These dimensions were determined from experimentation, material availability and by targeting the performance figures outlined earlier. The cross section size of each blade was 0.5×1.6 millimeter, and the spatial resolution of the array is 1.2×1.8 millimeter. To construct the array, piezoelectric bimorph plates were cut to a comb shape with 6 teeth as shown in Figure 4. The geometry was similar to that used in [15], but the dimensions were significantly revised due to following reasons.

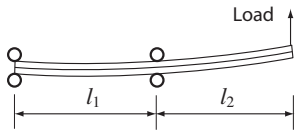

Figure 3: Dual pinned lever.

The clamping method was modified from a basic cantilever structure to a dual-pinned structure as shown in Figure 3. This is because we found that for a given material and a given a voltage, this structure had a compliance/free-deflection tradeoff able to cause skin deformation much larger than a basic cantilever structure [22]. With skin contactors 1.6 mm wide, the free maximum deflection had to be be no less than 0.1 mm and the blocked force had to be more than 0.125 N, according to our experimental data. In the same reference, we found that the compliance of a cantilever is $\propto [(l_1+l_2)l_2]^{3/2}$ which is always larger than that of the dual-pinned beam which is $\propto [(l_1+l_2){l_2}^2]$. After careful design, the optimal l_1 and l_2 were determined to be order of 20 mm and 10 mm respectively for the material we used.

The surface electrode was carefully removed in the area between each comb tooth, making them electrically independent. This resulted in "comb modules" which are illustrated in Figure 4, where electrical connections are provided by small independent printed circuits boards. Each piezoelectrical comb was bonded to these printed circuit boards with high performance epoxy to form a complete interchangeable module.

Looking at Figure 5, modules were assembled in a "fan" geometry which had the effect of creating a cradle of radius 25 mm in which the fingertip could rest with minimal pre-loading. To protect users from electrical shock, a thin layer of varnish was coated at the tip of each piezo tooth. Moreover, the surface electode within 0.5 mm from the each tooth tip was removed.

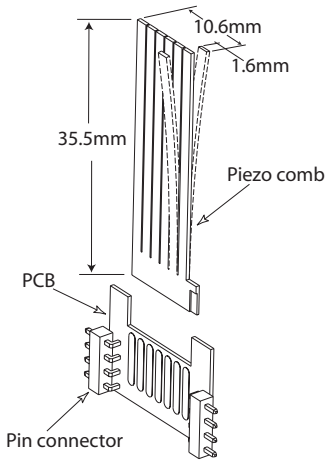

Figure 4: Single comb module.

4.2 Modularity

The actuator array is the most fragile and expensive part of the transducer. The entire transducer is illustrated in Figures 5 and 6. Each module was connected to two side-boards via two four-pin connectors. These side-boards have two functions. The first is structural mechanical support in the form of a stiff box structure needed to create the dual-pinned support for the benders. The second is to route voltage signal from the driving electronics located on the base motherboard (it also has electrical test pads for debugging). In addition, pre-drilled holes at certain places make it possible to change the ratio l_2/l_1 in a matter of minutes.

An assembled view of the whole system is seen in Figure 6 along with the connectors to a computer interface and to the power management unit.

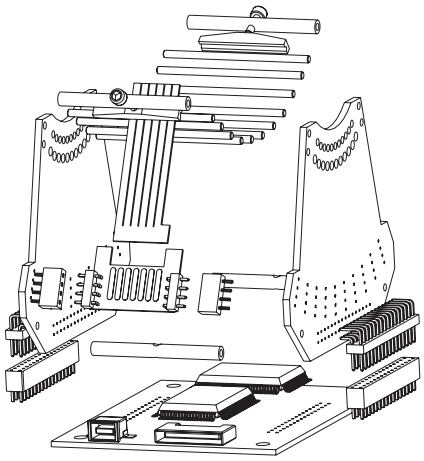

Figure 5: Exploded view.

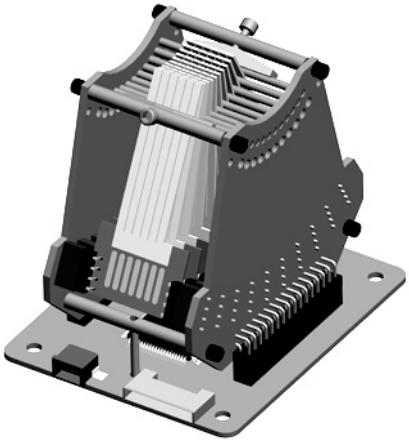

Figure 6: Assembled view.

4.3 Driving electronics

In order to maximize portability and reduce the number of connections, we applied the principle of time division to the greatest extent possible. For this, we used two HV257 chips (Supertex Inc., Sunnyvale, CA, USA). This chip is an integrated 32-channel sample/hold and high voltage amplifier. The system diagram is illustrated in some detail in Figure 7.

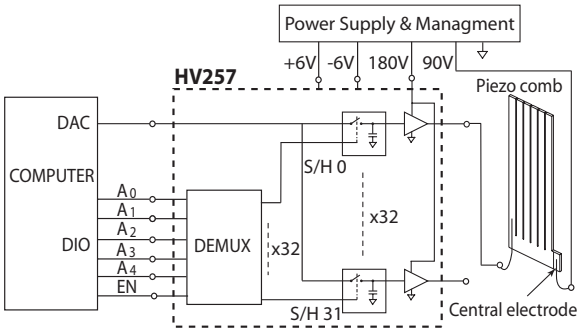

Figure 7: Driving electronics diagram.

Here, we used RTLinux™ to drive the system from a real-time clock. The software driver first sends a desired analog output through a DAC, then specifies the channel address of a high voltage amplifier. Each sample and hold could easily be refreshed at rate of 4 kHz. At this frequency, the electromechanical transfer function of the actuators could could act as a reasonably good reconstruction filter.

Since the HV257 operates unipolar amplifiers, we connected the central electrode of all piezo combs to a regulated 90 V center tap power rail and the amplifiers supplied voltages between 0 V and 180 V. The potential difference between the surface electrode and central electrode thus varied from -90 V to +90 V. Internal current limiters maked the system completely safe to use.

5 Results

5.1 Blocked force, Free deflection & Stiffness

To measure the deflection of a tooth, a tiny mirror was glued to it in order to reflect the beam of a laser. The reflected beam created a bright spot on a lateral position sensing detector (PSD, Model DL-10; UDT Sensors, Inc., Hawthorne, CA, USA) which after calibration gave the tooth deflection. To measure the free deflection, we applied several cycles of low frequency sinusoidal voltage of 90 V amplitude to an unloaded piezo tooth and recorded the deflection. It was 0.075 mm for $l_2 = 7.5$ mm, and 0.1 mm for $l_2 = 10.0$ mm.

To measure the blocked force, which we first applied the maximum voltage to one piezo tooth, and then applied an increasingly larger known tangential forces at the tip of the tooth until the deflection was zeroed. The blocked force produced by each tooth was 0.22 N for $l_2 = 7.5$ mm, and 0.15 N for $l_2 = 10.0$ mm.

The stiffness was measured by measuring the relationship between deflections and applied forces. The setup was similar to that used to measure the blocked force, but no voltage was applied to the piezo tooth. Figure 8 collects the results which are consistent with the other experiments (a shorter l_2 yields a stiffer tooth).

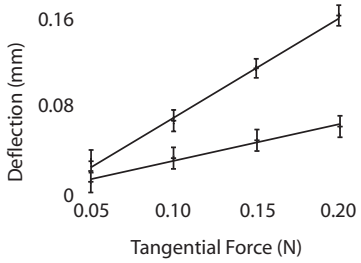

Figure 8: Measured tooth deflection for two different l_2/l_1 ratios.

5.2 System bandwidth

The free displacement frequency response of a tooth was measured by sweeping an input signal between 30 Hz to 2000 Hz and measuring the response. The results, see Figure 9, show that the system bandwidth is larger than 250 Hz. The actuator resonates at about 1500 Hz when $l_2 = 10$ mm, and at 1750 Hz when $l_2 = 7.5$ mm. In both cases, this frequency is far above the targeted operating range. The amplitude roll-off starting at about 250 Hz can be attributed to a combination of internal dissipation in the piezo-electric material and losses in the hinges (presently made of thermoplastic sheathes heat-shrunk around stiff ceramic rods).

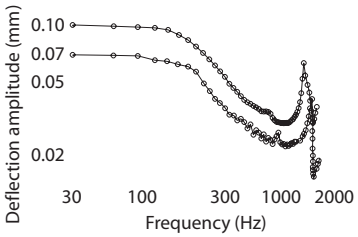

Figure 9: Measured bode plot for different l_2/l_1 ratios.

6 Pilot experiment

To validate the initial functionality of the tactile display, a simple psychophysical experiment was conducted. In this experiment, 6 healthy, right-handed subjects (2 females and 4 males; age: 26-33) volunteered to participate. They were asked to detect a virtual line of 2 mm width. We sought to find a preliminary estimate of the threshold of stimuli intersity in terms of the voltage applied to the piezo teeth, that could be easily detected.

6.1 Protocol

The tactile transducer was mounted to a Pantograph haptic device as shown in Figure 10 [3], which was used as a frictionless carrier and a position detector. A computer recorded the movements of the tactile transducer in the horizontal place with a resolution of 10 μm when it was moved about by the subject.

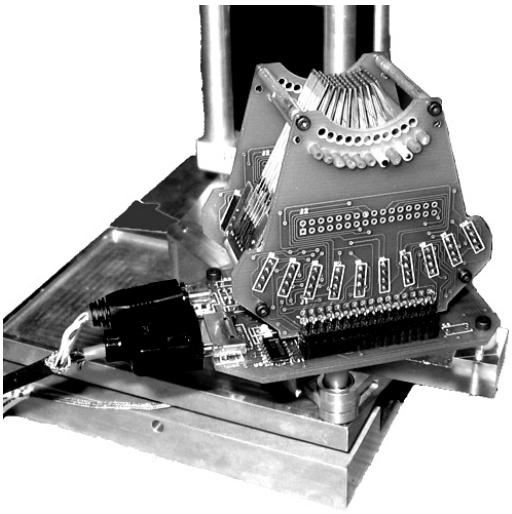

Figure 10: Psychophysical experiment setup

A virtual line parallel to the medial axis of thickness $2l$, $l =$ 1 mm, was generated by the computer and randomly located along frontal direction within the workspace of the Pantograph (10 cm). The computer acquired the position of the tactile transducer and calculated the position of each tooth. The voltage applied to each tooth was determined according to its relative position to the virtual line $x_{\text{tooth}} - x_{\text{line}}$. When a given tooth was on the left of the line, the voltage applied to the piezoelectric tooth was set to be $90 + V_{\text{trial}}$; when the tooth is on the right of the bump, the voltage applied was set to be $90 - V_{\text{trial}}$, with a smooth transition in between when $-l < (x_{\text{tooth}} - x_{\text{line}}) < +l$:

$$V_{\text{applied}} = V_{\text{trial}} \cos\left(\frac{\pi}{2}\frac{x_{\text{tooth}} - x_{\text{line}}}{l}\right) + 90 \qquad (1)$$

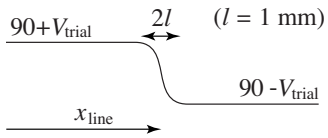

Figure 11: Voltage applied to actuator.

At the start of the trials, subjects were seated comfortably in front of the apparatus, and had their index resting on the active surface of the tactile transducer array. During the trials, subjects gently explored the virtual surface to localize the virtual line. The velocity of the movement was always smaller than 50 mm/s. As soon as subjects thought they had found the virtual line, they were instructed to move the center of the tactile array to that position and press the space bar of the computer keyboard. The computer randomly generated x_{line}, and V_{trial} was randomly set among the values 2.5, 5.5, 9.5, 12, 15, 18, 21, 25, 28, and 31 V. Each subject performed 50 trials. An answer was considered to be correct when the position at which subjects localized the line was within $x_{\text{line}} \pm 7.5$ mm. This value was selected because the test was detection, not localization, yet it allowed to reject accidental detections.

6.2 Results & Discussion

Figure 12 summarizes the averaged results. The performance was low when the voltage was smaller than 15 V which can be estimated to be the threshold. When the voltage was sufficiently high (25 V), the percentage of correct answers was close to 100%.

These results are preliminary since the experiment was intended to demonstrate functionality of the device at its most basic level, that is, was the device able to generate a detectable signal. The result suggests that this is the case for at least one signal and for an amplitude that was roughly 20% of the total available signal amplitude.

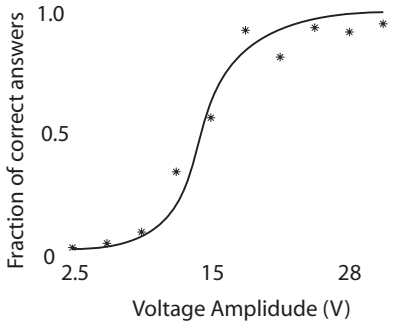

Figure 12: Virtual line localization results.

7 Conclusion and future work

This paper described a new, modular, high-performance, tactile transducer device based on lateral skin deformation. It had 60 actuators creating an active surface of about 10 mm^2 in the shape of a cradle designed to minimize the finger pre-load when the tactile signals is quiescent. The system is compact (150 cm^2, 60 g) and has integrated electronics requiring a small number of connection wires for operation. A prominent feature the device is the ease with which is can be fabricated and serviced.

The results indicated that each actuator could produce a free deflection of 0.1 mm and a blocked force of 0.15 N (or 0.075 mm and

0.22 N) figures which appear to be capable of creating large deformation in 1.6×1.0 mm patches of the fingertip skin for most users. The system bandwidth is high, more than 250 Hz, making the system not only promising for the creation of the sensations of small shapes, but also of fine textures.

A pilot test indicated that the threshold of creation of a tactile sensation at a single site is in the vicinity of 15 V, while the maximum activation voltage can be up to 90 V, allowing for significant headroom in the delivery of tactile signals.

Our present efforts are directed at further characterization of the device and at the development of a variety of activation patterns designed to explore the range of the sensation that can be created with this technology.

ACKNOWLEDGMENTS

The authors are deeply indebted to Jérôme Pasquero and Vincent Levesque of the Haptics Laboratory at McGill University whose research in closely related problems was instrumental in motivating us to developing this new prototype device.

This research was supported IRIS, the Institute for Robotics and Intelligent Systems. Qi Wang would like to thank McGill University for an Eric L. Adler Fellowship in Electrical Engineering and Vincent Hayward would like to thank NSERC, the Natural Sciences and Engineering Research Council of Canada, for a Discovery Grant.

REFERENCES

[1] J. Biggs and M. A. Srinivasan. Tangential versus normal displacements of skin: Relative effectiveness for producing tactile sensations. In *Proc. of the 10th International Symposium on Haptic Interfaces for Virtual Environment and Teleoperator Systems*, pages 121–128, 2002.

[2] J. Bliss, M. Katcher, C. Rogers, and R. Shepard. Optical-to-tactile image conversion for the blind. *IEEE Transactions on Man-Machine Systems*, 11:58–65, 1970.

[3] G. Campion, Q. Wang, and V. Hayward. The Pantograph Mk-II: A haptic instrument. In *Proc. IROS 2005, IEEE/RSJ Int. Conf. Intelligent Robots and Systems*, pages 723–728, 2005.

[4] K. Drewing, M. Fritschi, R. Zopf, M. Ernst, and M. Buss. First evaluation of a novel tactile display exerting shear force via lateral displacement. *ACM Transactions on Applied Perception*, 2(2):118–131, 2005.

[5] R. Ghodssi, D. J. Beebe, V. White, and D. D. Denton. Development of a tangential tactor using a liga/mems linear microactuator technology. In *MicroElectro-Mechanical Systems (MEMS) 1998 International Mechanical Engineering Congress and Exposition*, 1998. .

[6] V. Hayward and M. Cruz-Hernandez. Tactile display device using distributed lateral skin stretch. In *Proc. of the Haptic Interfaces for Virtual Environment and Teleoperator Systems Symposium (IMECE2000)*, volume DSC-69-2, pages 1309–1314. ASME, 2000.

[7] T. Iwamoto and H. Shinoda. Ultrasound tactile display for stress field reproduction – examination of non-vibratory tactile apparent movement. In *Proc. of the First Joint Eurohaptics Conference and Symposium on Haptic Interfaces for Virtual Environment and Teleoperator Systems WHC'05*, pages 220–228, 2005.

[8] M. Jungmann and H. F. Schlaak. Miniaturised electrostatic tactile display with high structural compliance. In *Eurohaptics 2002*, 2002.

[9] M. B. Khoudja, M. Hafez, J.-M. Alexandre, A. Kheddar, and V. Moreau. VITAL: A new low-cost vibro-tactile display system. In *Proc. IEEE International Conference on Robotics & Automation*, pages 721–726, 2004.

[10] R. Kikuuwe, A. Sano, H. Mochiyama, N. Takesue, and H. Fujimoto. Enhancing tactile perception of surface undulation. *ACM Transactions on Applied Perception*, 2(1):46–67, 2005.

[11] M. Konyo, S. Tadokoro, T. Takamori, and K. Oguro. Artificial tactile feel display using soft gel actutators. In *Proc. IEEE International Conference on Robotics & Automation*, pages 3416–3421, 2000.

[12] V. Levesque and V. Hayward. Experimental evidence of lateral skin strain during tactile exploration. In *Proc. Eurohaptics 2003*, pages 261–275, 2003.

[13] V. Levesque, J. Pasquero, V. Hayward, and M. Legault. Display of virtual Braille dots by lateral skin deformation: Feasibility study. *ACM Transactions on Applied Perception*, 2(2), 2005.

[14] G. Moy, C. Wagner, and R. S. Fearing. A compliant tactile display for teletaction. In *Proc. IEEE Int. Conf. on Robotics and Automation*, pages 3409–3415, 2000.

[15] J. Pasquero and V. Hayward. STRESS: A practical tactile display system with one millimeter spatial resolution and 700 Hz refresh rate. In *Proc. Eurohaptics 2003*, pages 94–110, 2003.

[16] I. Sarakoglou, N.Tsagarakis, and D.G.Caldwell. A portable fingertip tactile feedback array – transmission system reliability and modelling. In *Proc. of the First Joint Eurohaptics Conference and Symposium on Haptic Interfaces for Virtual Environment and Teleoperator Systems WHC'05*, pages 547–548, 2005.

[17] I. R. Summers and C. M. Chanter. A broadband tactile array on the fingertip. *J. Acoustical Society of America*, 112:2118–2126, 2002.

[18] H. Tang and D.J. Beebe. A microfabricated electrostatic haptic display for persons with visual impairments. *IEEE Transactions on rehabilitation engineering*, 6(3):241–248, 1998.

[19] N.G. Tsagarakis, T. Horne, and D. G. Caldwell. Slip aestheasis: A portable 2d slip/skin stretch display for the fingertip. In *Proc. of the First Joint Eurohaptics Conference and Symposium on Haptic Interfaces for Virtual Environment and Teleoperator Systems WHC'05*, pages 214–219, 2005.

[20] R. Velazquez, E. Pissaloux, M. Hafez, and J. Szewczyk. A low-cost highly-portable tactile display based on shape memory alloy micro-actuators. In *VECIMS 2005, IEEE International Conference on Virtual Environments, Human-Computer Interfaces, and Measurement Systems*, 2005.

[21] C.R. Wagner, S.J. Lederman, and R.D. Howe. Design and performance of a tactile shape display using RC servomotors. *Haptics-e*, 3(4), 2004.

[22] Q. Wang and V. Hayward. In vivo biomechanics of the fingerpad skin under local tangential traction. *Submitted*, 2005.

[23] R. J. Webster III, T. E. Murphy, L. N. Verner, and A. M. Okamura. A novel two-dimensional tactile slip display: design, kinematics and perceptual experiments. *ACM Transactions on Applied Perception*, 2(2):150–165, 2005.

[24] P. Wellman, W. Peine, G. Favalora, and R. Howe. Mechanical design and control of a high-bandwidth shape memory alloy tactile display. In A. Casals and A. T. de Almeida, editors, *Experimental Robotics V, Lecture Notes in Control and Information Science 232,*, pages 56–66. Springer Verlag, 1998.